Heat Transfer Intensity Analysis in Varied Combustion Reaction Mechanism Steps.

R.S. Lebelo[1*], S.O. Adesanya[1,2], A.T. Adeosun[3], T.A. Yusuf[4] and S.O. Akindeinde[5]

[1]Department of Applied Physical Sciences, Vaal University of Technology, Vanderbijlpark,South Africa
[2]Department of Mathematics and Statistics, Redeemer's University, Ede, Nigeria.
[3]Department of Mathematics, Federal College of Education, Iwo, Nigeria.
[4]Department of Mathematics, Adeleke University, Ede, Nigeria.
[5]Department of Mathematics and Statistical Sciences, Botswana International University of Science and Technology, Palapye, Botswana.

Abstract: *This article investigates the intensity of heat transfer in reaction mechanisms involving differentiated steps of the combustion process. Three scenarios are considered, which include a one-step, two-step, and three-step combustion reaction mechanisms. Three steady-state energy equations involving, respectively, assumed one-step, two-step, and three-step reaction mechanisms in reactive combustible materials modelled in a cylindrical domain were numerically analysed to demonstrate how the intensity of heat transfer occurs as combustion takes place in a multiple-step reaction mechanism. The study is theoretical and applies a nonlinear differential equation that is solved by numerical methods, and in this case, the Runge-Kutta Fehlberg method (RKF45) coupled with the Shooting Technique was used to solve the equation, and the results were obtained through Maple software. The use of parameters such as the reaction rate, activation energy, and radiation indicated that the temperature profiles are of the highest magnitude in a three-step reaction mechanism compared to the two-step and one-step reactions.*

Keywords: Heat transfer, multi-step, reaction mechanism, cylindrical domain, numerical methods.

Nomenclature

A_1, A_2, A_3	Rate constant $[\mathrm{s}^{-1}]$, (respective steps 1, 2, 3)
Q_1, Q_2, Q_3	Heat of reaction $[\mathrm{Jkg}^{-1}]$, (respective steps 1, 2, 3)
E_1, E_2, E_3	Activation energy $[\mathrm{Jmol}^{-1}]$, (respective steps 1, 2, 3)
h	Heat transfer coefficient $[\mathrm{Js}^{-1}\mathrm{m}^{-1}\mathrm{K}^{-1}]$
k	Thermal conductivity $[\mathrm{Js}^{-1}\mathrm{m}^{-1}\mathrm{K}^{-1}]$
K	Boltzmann constant $[\mathrm{JK}^{-1}]$
l	Planck number [Js]
m	Numerical exponent
R	Universal gas constant $[\mathrm{JK}^{-1}\mathrm{mol}^{-1}]$
Ra	Radiation parameter
T	Absolute temperature of the cylinder [K]
T_S	Surface temperature of the cylinder [K]

$\bar{r}$ Cylinder's rectangular distance [m]
r Dimensionless distance
v Vibration frequency [s^{-1}]

Greek Symbols

γ, μ Dimensionless energy ratio parameters (respective steps 2, 3)
β, δ Dimensionless exothermic chemical reaction parameters (respective steps 2, 3)
φ Dimensionless activation energy parameter
θ Dimensionless temperature
α Emissivity of the slab
λ Modified Frank-Kamenetskii parameter
σ Stefan-Boltzmann constant [W/m^2K^4]

1. INTRODUCTION

The study of heat transfer has attracted numerous researchers due to its diverse applications in real-life situations. Significant work has been conducted on heat transfer studies in both one-step and two-step reaction mechanisms of combustible materials within a cylindrical domain. Adeosun et al. [1] investigated the combustion of visco-electrical material with oxygen consumption within a cylindrical stockpile, where a two-step reaction mechanism was assumed. Their study agreed with the work done in [2,3], emphasising that spontaneous combustion in reactive materials occurs due to exothermic chemical reactions when the carbon-containing materials react spontaneously with the oxygen trapped within a stockpile of such materials. This phenomenon was also studied in [4], where heat transfer analysis was investigated in a convective reactive stockpile in a cylindrical domain, and in [5], a one-step heat transfer stability with carbon dioxide emission in a stockpile of reactive materials was also modelled in a cylindrical pipe was analysed. In all the mentioned studies, it was demonstrated that the temperature of the combustion system intensified with an increase in the magnitude of the reaction rate parameter. Chinyoka and Makinde [6] studied thermal decomposition in a cylindrical domain with carbon dioxide emission and oxygen depletion. Their study was based on a one-step chemical reaction mechanism where the emphasis on the temperature rise in a combustible material was demonstrated by increasing factors such as the reaction rate and reaction kinetics type. Furthermore, the study of combustible material in a cylindrical domain for a one-step chemical reaction was also done in [7], where it was demonstrated that a combustible material with variable thermal conductivity enhances thermal decomposition as compared to a constant thermal conductivity condition. Thermal conductivity is very important in the study of heat transfer, and its applications in engineering include the following, for example, generation of power, harvesting and storing of energy, processing of material, and in electronics, it is used for thermal management [8]. Furthermore, heat transfer applications are outlined in [9] and include, among others, the processing of hydrocarbons, which involve the processing of oil and gas, purification of natural gas, processing of asphalt and its storage, and the processing of plastics, which involve the moulding

of plastic, manufacturing of the following, synthetic fibre, plastics and polymer and specialty polymer that is heat sensitive.

The previous studies done in heat transfer processes used a one and two-step low oxidation chemical reaction. A comparison of the heat transfer in media of different physical geometries was done in [10], where it was demonstrated that heat transfer in spherical domains is more stable as compared to cylindrical and rectangular domains. The difference in this case is that heat transfer differentiation is studied in three scenarios, namely, one, two, and three-step low-temperature chemical reactions. To the knowledge of the authors, this study has not been demonstrated before.

2. MATERIALS AND METHODS

2.1 Problem Formulation

The study of the heat transfer intensity of reactive materials is modelled in a cylindrical domain, as indicated by Figure 1. A one-dimensional energy equation is applied with the assumption that the reactive material's thermal conductivity is constant. The geometry of the problem is given as follows:

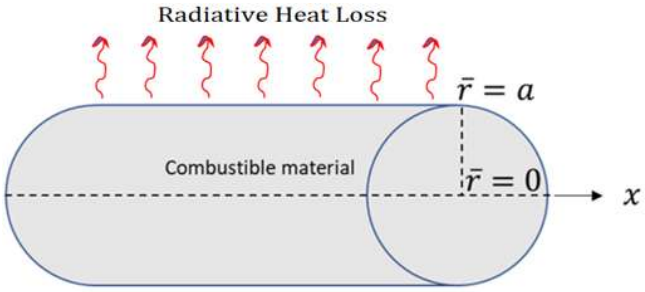

Figure 1. Geometry of the problem

A complete combustion in a one, two, and three-step low oxidation chemical reaction is assumed in this study, and following [12, 13], the energy formula, with radiative heat loss, for the respective one-step and two-step low-temperature oxidation reaction mechanism, is represented, as follows,

$$\frac{k}{\bar{r}}\frac{d}{d\bar{r}}\left(\bar{r}\frac{dT}{d\bar{r}}\right) + Q_1A_1\left(\frac{KT}{vl}\right)^m e^{-E_1/RT} - \mu\sigma(T^4 - T_w^4) = 0, \quad (1)$$

$$\frac{k}{\bar{r}}\frac{d}{d\bar{r}}\left(\bar{r}\frac{dT}{dr}\right) + Q_1A_1\left(\frac{KT}{vl}\right)^m e^{-E_1/RT} + Q_2A_2\left(\frac{KT}{vl}\right)^m e^{-E_2/RT} - \mu\sigma(T^4 - T_w^4) = 0. \quad (2)$$

The energy equation for the three-step low temperature oxidation reaction mechanism is presented in equation 3 below.

$$\frac{k}{\bar{r}}\frac{d}{d\bar{r}}\left(\bar{r}\frac{dT}{d\bar{r}}\right) + Q_1A_1\left(\frac{KT}{vl}\right)^m e^{-E_1/RT} + Q_2A_2\left(\frac{KT}{vl}\right)^m e^{-E_2/RT} + Q_3A_3\left(\frac{KT}{vl}\right)^m e^{-E_3/RT} +$$

$$-\mu\sigma(T^4 - T_w^4) = 0. \quad (3)$$

The boundary conditions for the first and the second ends are described as,

$$\frac{dT}{d\bar{r}}(0) = 0;\ \ T(a) = T_w. \tag{4}$$

The dimensional parameters are described here, where $Q_1, A_1, E_1, R,$ are respectively the heat of reaction, the rate constant, the activation energy for the step-1 reaction mechanism, and the universal gas constant. The Planck number, vibration frequency, and Boltzmann constant are represented by $l, v, K.$ m is for the chemical reaction kinetics type, where $m = -2$ represents the sensitized, $m = 0$ the Arrhenius, and $m = 0.5$ the bimolecular kinetics, and $\bar{r}$ is the radial distance. Furthermore, k represents the material's thermal conductivity, Q_2, A_2 are for the heat of reaction, and rate constant, respectively, for the step-2 reaction mechanism. In addition, Q_3, A_3 are respectively the heat of reaction and the rate constant for the step-3 reaction mechanism. E_1, E_2 and E_3 are the respective activation energies for the step-1, step-2, and step-3 reaction mechanisms. It should be noted further that T represents the cylinder's absolute temperature, and T_w the surrounding temperature. Radiative heat loss is represented by Stefan-Boltzmann's law, presented as $q = \mu\sigma(T^4 - T_w^4)$, where μ represents the cylinder's emissivity, and σ the constant for Stefan-Boltzmann.

2.2 Dimensionless Parameters Introduction

To solve the equations (1-4) numerically, it is convenient to change them into dimensionless form, which is done as follows, starting with equation (1):

$$\theta = \frac{E(T-T_w)}{RT_w^2}, r = \frac{\bar{r}}{a}, \quad \varphi = \frac{RT_w}{E}, Ra = \frac{\mu\sigma E a^2 T_w^2}{kR}, \lambda = \left(\frac{KT_w}{vl}\right)^m \frac{QAEa^2}{kRT_w^2} exp\left(-\frac{E}{RT_w}\right). \tag{5}$$

For equation (2):

$$\theta_1 = \frac{E_1(T-T_w)}{RT_w^2}, r = \frac{\bar{r}}{a}, \varphi_1 = \frac{RT_w}{E_1}, \alpha = \frac{E_2}{E_1}, \beta = \frac{Q_2A_2E_2}{Q_1A_1E_1} e^{(E_1-E_2)/RT}, Ra_1 = \frac{\mu\sigma\ {}_1 a^2 T_W^2}{kR},$$

$$\lambda = \left(\frac{KT_w}{vl}\right)^m \frac{Q_1A_1E_1a^2}{kR\ {}_w^2} exp\left(-\frac{E_1}{RT_w}\right). \tag{6}$$

For equation (3):

$$\theta_2 = \frac{E_2(T-T_W)}{RT_W^2}, \beta = \frac{Q_2A_2E_2}{Q_1A_1E_1} e^{(E_1-E_2)/RT}, \alpha = \frac{E_2}{E_1}, \beta_1 = \frac{Q_3A_3E_3}{Q_2A_2E_2} e^{(E_2-E_3)/RT}, \alpha_1 = \frac{E_3}{E_2}, r = \frac{\bar{r}}{a},$$

$$\varphi_2 = \frac{RT_W}{E_2}, Ra_2 = \frac{\mu\sigma\ {}_2 a^2 T_W^2}{kR}, \lambda = \left(\frac{KT_W}{vl}\right)^m \frac{Q_1\ A_1E_1\ a^2}{kRT_W^2} exp\left(-\frac{E_1}{RT_W}\right). \tag{7}$$

In equations (5-7), the dimensionless parameters are described as follows, where $\theta, \theta_1, \theta_2,$ are the dimensionless temperatures for the respective steps, λ is the Frank-Kamenetskii parameter, also called the reaction rate parameter, $\varphi, \varphi_1, \varphi_2,$ are the respective dimensionless activation energy parameters for the three steps, r is the dimensionless radial distance, $\alpha, \alpha_1,$ are the activation energy ratio parameters for the second and third steps, β, β_1 are the two-step low-temperature oxidation parameters for the second and third steps, and Ra, Ra_1, Ra_2 are the dimensionless radiation parameters for the three steps.

The dimensionless equations (1-3) take the respective forms

$$\frac{1}{r}\frac{d}{dr}\left(r\frac{d\theta}{dr}\right)+\lambda(1+\varphi\theta)^m e^{\theta/(1+\varphi\theta)}-Ra[(\varphi\theta+1)^4-1]=0, \quad (8)$$

$$\frac{1}{r}\frac{d}{dr}\left(r\frac{d\theta_1}{dr}\right)+\lambda(1+\varphi_1\theta_1)^m\left\{e^{[\theta_1/(1+\varphi_1\theta_1)]}+\beta e^{[\alpha\theta_1/(1+\varphi_1\theta_1)]}\right\}-Ra_1[(\varphi_1\theta_1+1)^4-1]=0, \quad (9)$$

$$\frac{1}{r}\frac{d}{dr}\left(r\frac{d\theta_2}{dr}\right)+\lambda(1+\varphi_2\theta_2)^m e^{[\theta_2/(1+\varphi_2\theta_2)]}+\lambda\beta(1+\varphi_2\theta_2)^m e^{[\alpha\theta_2/(1+\varphi_2\theta_2)]}+\lambda\beta_1(1+\varphi_2\theta_2)^m e^{[\alpha_1\theta_2/(1+\varphi_2\theta_2)]}-Ra_2[(\varphi_2\theta_2+1)^4-1]=0. \quad (10)$$

The boundary conditions are

$$\frac{d\theta}{dr}(0)=0;\ \ \theta(1)=0. \quad (11)$$

3. NUMERICAL PROBLEM SOLUTION

The Runge-Kutta-Fehlberg (RKF45) method, coupled with the Shooting technique, was applied to numerically solve the energy equations (8-11). It is necessary to establish the convergence of the RKF45, and equation (10) was used for the purpose of plotting Figure 2, which demonstrates the convergence of the solution and confirms that the temperature will ultimately reduce to zero (0) as the domain increases to infinity.

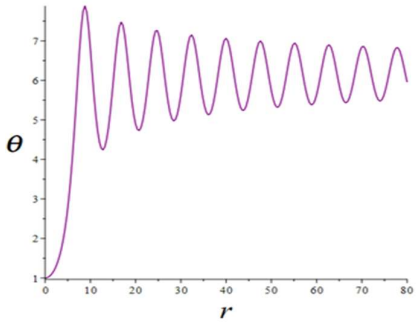

Figure 2. Solution Convergence

Table 1 shows that increasing the step size ***h*** from 0.0001 to 2.5 corresponds to an increase in the error (E). This scenario confirms that it is necessary to keep the step size very low to attain the accuracy of the solution.

Table 1. RKF45 Convergence

h	**E**
0.0001	1.7×10^{-13}
0.0010	1.667×10^{-10}
0.0100	1.66666×10^{-7}
0.1000	0.00016658335
1.0000	0.1585290152
1.5000	0.5025050134
2.0000	1.090702573
2.5000	1.901527856

Figure 3 below demonstrates the increase in error (E) as the step size varies from 0.0001 to 2.

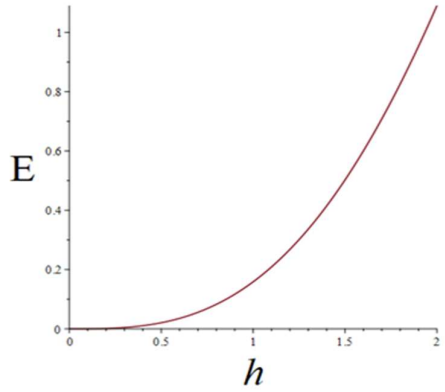

Figure 3. Step size increase with error increase

The following algorithms for each equation were obtained, where, for convenience, $\theta = \theta_1 = \theta_2 = g_1,\ g_1{}' = g_2$ and $g'_2 = g_3$.

Equations (8-11) respectively took the forms represented by equations (12-15)

$$g_3 = -g_2 - \lambda(1+\varphi g_1)^m e^{g_1/(1+\varphi g_1)} + Ra((\varphi g_1 + 1)^4 - 1) \quad (12)$$

$$g_3 = -g_2 - \lambda(1+\varphi_1 g_1)^m e^{g_1/(1+\varphi_1 g_1)} - \lambda\beta(1+\varphi_1 g_1)^m e^{[\alpha g_1/(1+\varphi_1 g_1)]} + Ra_1((\varphi_1 g_1 + 1)^4 - 1) \quad (13)$$

$$g_3 = -g_2 - \lambda(1+\varphi_2 g_1)^m e^{g_1/(1+\varphi_2 g_1)} - \lambda\beta(1+\varphi_2 g_1)^m e^{[\alpha g_1/(1+\varphi_2 g_1)]} - \lambda\beta_1(1+\varphi_2 g_1)^m e^{[\alpha_1 g_1/(1+\varphi_2 g_1)]} + Ra_2((\varphi_2 g_1 + 1)^4 - 1) \quad (14)$$

The boundary conditions take the form

$$g_2(0) = 0,\ g_1(1) = 0 \quad (15)$$

Maple software was used to solve problems numerically, resulting in graphical solutions, and their discussions are given in the following section.

4. RESULTS AND DISCUSSION

The following kinetic parameters $\lambda = 0.1, m = 0.5, Ra = 1, \varphi = 0.1,$ were conveniently used to study the behaviours of temperature profiles in different steps of reaction mechanisms, to gain an understanding of the varied radiative heat transfer in each step.

4.1 Temperature Profiles Discussion

Figures 4 (a)-(c) indicate the effects of the reaction rate parameter (λ), on the temperature of the system in the one-step, two-step, and three-step low-temperature oxidation reaction mechanism, respectively. It can be observed that the profiles of the temperature are increased as the λ is increased, confirming that λ enhances the low-temperature oxidation process. The focus of the study is to check the profiles of the temperature in each reaction mechanism step. For example, when $\lambda = 0.4$, the highest profiles are observed for all the steps and it should be noted that for a one-step combustion process, $\lambda = 0.4$ gives the highest value of the temperature $\theta = 0{,}10057$, for the two-step, $\lambda = 0.4 \Rightarrow \theta = 0.11077$, and for the three-step condition, the $\lambda = 0.4 \Rightarrow \theta = 0.121$, as shown in Tables 2(a)-(c). Since $\theta = 0.121 > 0.11077 > 0.10057$, it is clear that the low-temperature oxidation chemical reaction mechanism intensifies from a one-step to a three-step one. This accounts for a complete combustion process in a multi-step reaction mechanism. The same scenario is depicted in Figures 5(a)-(c), where the reaction kinetics type (m), shows an increase in the temperature profiles as m's magnitude varies from -2 to 0.5. When $m = -2; 0; 0.5$ in a one-step combustion process, the corresponding temperature values were calculated as $\theta = 0.4493; 0.49728; 0.51162$, and for the two-step condition, $m = -2; 0; 0.5$ gave the temperatures $\theta = 0.4943; 0.55269; 0.57083$. Lastly, the three-step combustion process for $m = -2; 0; 0.5$ resulted in the temperature values $\theta = 0.53882; 0.60941; 0.63203$. All these values are displayed in Tables 3(a)-(c). It should also be noted that for $m = 0.5$, as an example, in one-step, two-step, and three-step reaction mechanisms, the respective different magnitude values of the temperature are $\theta = 0.5116 < 0.57083 < 0.63203$. This argument also confirms that the temperature intensifies in a multi-step combustion process. A different scenario is observed in Figures 6(a)-(c) and 7(a)-(c), where the respective increase in the radiation parameter (Ra) and the activation energy parameter (φ), show a decline in the temperature profiles. The decline in the temperature profiles indicates that the parameters retard the intensity of the temperature rise during the combustion process. The profiles also indicate that the temperature intensifies as the combustion process occurs in a multi-step condition. As indicated previously, for example, $Ra = 4$ shows that the temperature values in a one-step, two-step, and three-step reaction mechanism, as illustrated in Figs. 6(a)-(c), are respectively given by $\theta = 0.01945 < 0.02139 < 0.02334$. The temperature intensity is the highest in a three-step chemical reaction mechanism. For $\varphi = 0.4$ in the three steps illustrated by Figs. 7(a)-(c), the increasing temperature values are $\theta = 0.01945 < 0.02141 < 0.02336$. More temperature values calculated for one, two, and three-step combustion processes are depicted in Tables 4(a)-(c) and 5(a)-(c).

4.2 Temperature Profiles Figures

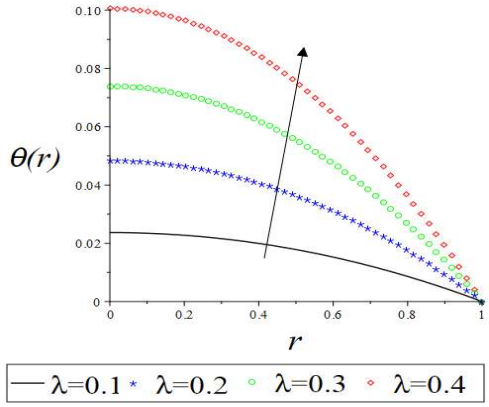

Figure 4(a). One-step mechanism

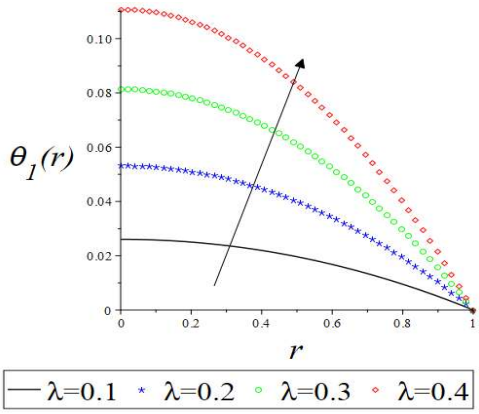

Figure 4(b). Two-step mechanism

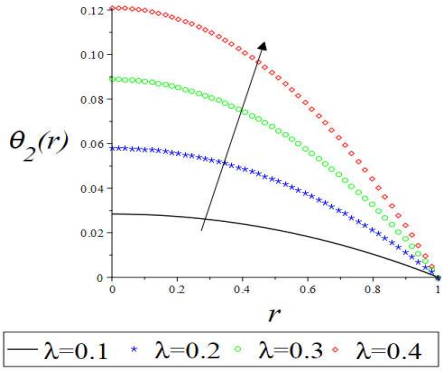

Figure 4(c). Three-step mechanism

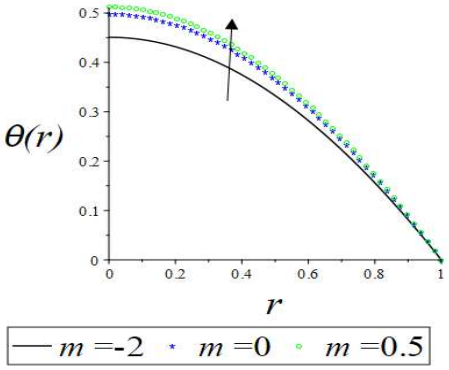

Figure 5(a). One-step mechanism

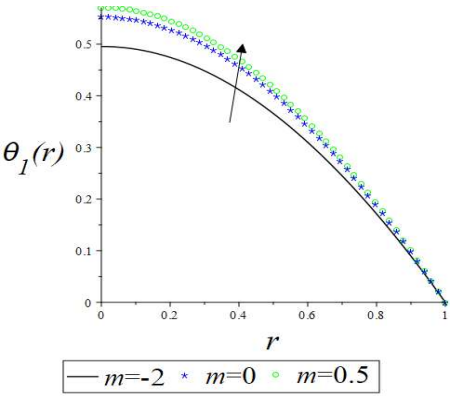

Figure 5(b). Two-step mechanism

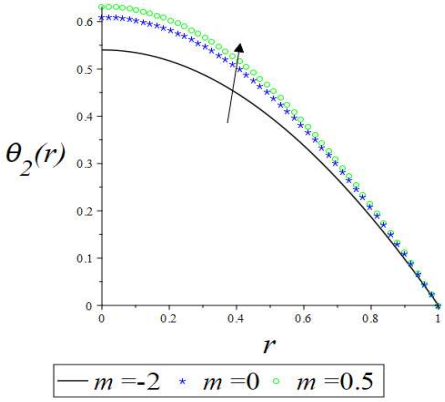

Figure 5(c). Three-step mechanism

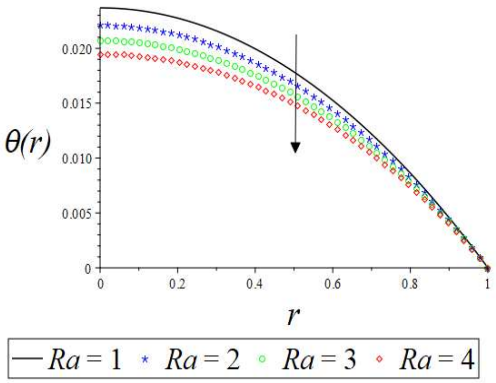

Figure 6(a). One-step mechanism

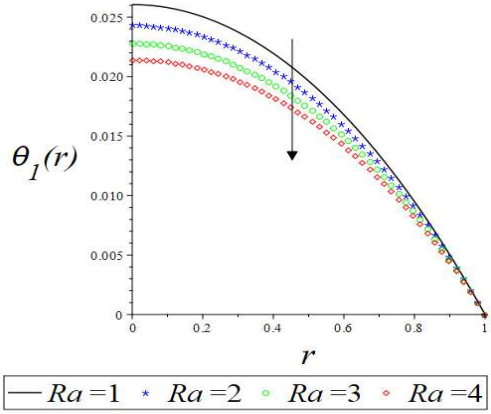

Figure 6(b). Two-step mechanism

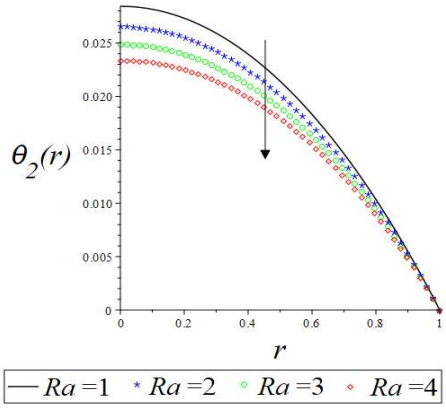

Figure 6(c). Three-step mechanism

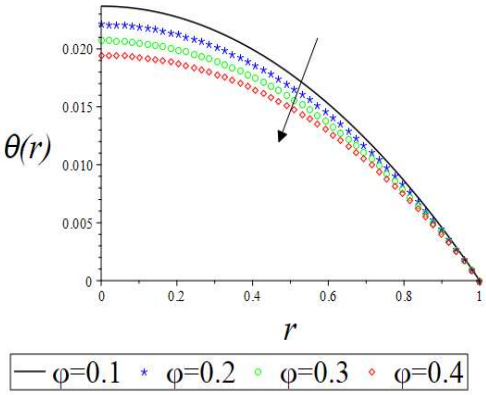

Figure 7(a). One-step mechanism

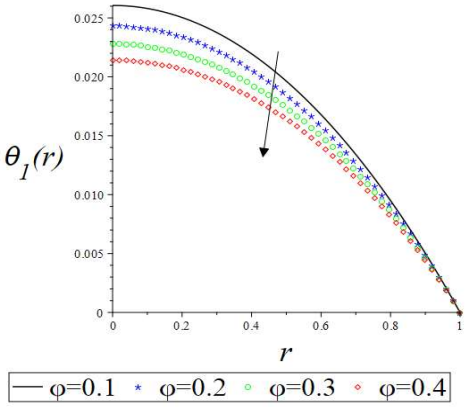

Figure 7(b). Two-step mechanism

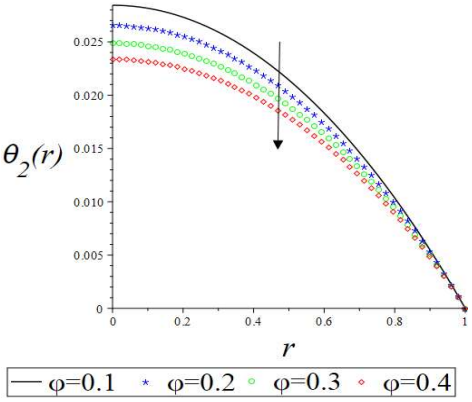

Figure 7(c). Three-step mechanism

4.3 Temperature Profiles Values

The values for the temperature profiles are provided in the table below.

Table 2(a). λ on Temperature (Fig. 4(a))

λ variation	θ values
0.1	0.02362
0.2	0.04829
0.3	0.07389
0.4	0.10057

Table 2(b). λ on Temperature (Fig. 4(b))

λ variation	θ_1 values
0.1	0.02599
0.2	0.05315
0.3	0.08135
0.4	0.11077

Table 2(c). λ on Temperature (Fig. 4(c))

λ variation	θ_2 values
0.1	0.02599
0.2	0.05315
0.3	0.08135
0.4	0.11077

Table 3(a). m on Temperature (Fig. 5(a))

m variation	θ values
-2	0.44935
0	0.49728
0.5	0.51162

Table 3(b). m on Temperature (Fig. 5(b))

m variation	θ_1 values
-2	0.4943
0	0.55269
0.5	0.57083

Table 3(c). m on Temperature (Fig. 5(c))

m variation	θ_2 values
-2	0.53882
0	0.60941
0.5	0.63203

Table 4(a). Ra on Temperature (Fig. 6(a))

Ra variation	θ values
1	0.0236
2	0.02209
3	0.02069
4	0.01945

Table 4(b). Ra on Temperature (Fig. 6(b))

Ra variation	θ_1 values
1	0.02599
2	0.02431
3	0.02276
4	0.02139

Table 4(c). Ra on Temperature (Fig. 6(c))

Ra variation	θ_2 values
1	0.02837
2	0.02652
3	0.02484
4	0.02334

Table 5(a). φ on Temperature (Fig. 7(a))

φ variation	θ values
0.1	0.0236
0.2	0.0221
0.3	0.0207
0.4	0.01945

Table 5(b). φ on Temperature (Fig. 7(b))

φ variation	θ_1 values
0.1	0.02599
0.2	0.02431
0.3	0.02276
0.4	0.02139

Table 5(c). φ on Temperature (Fig. 7(c))

φ variation	θ_2 values
0.1	0.02837
0.2	0.02652
0.3	0.02484
0.4	0.02334

5. CONCLUSION

In this article, a comparison of low-temperature oxidation reactions in three scenarios of the combustion process was investigated. This was done by comparing the temperature profiles affected by selected parameters. With the help

of the reaction rate parameter (λ), reaction kinetics type parameter (m), radiation parameter (Ra), and activation energy parameter (φ), it was possible to demonstrate how the temperature intensity strengthens from a one-step, two-step to a three-step combustion process, meaning that heat transfer increases as a multi-step low-temperature reaction mechanism takes place. In other words, heat transfer is increased as a complete combustion process takes place. It was also demonstrated that the parameters λ and m increase the intensity of heat transfer as their magnitudes are increased. On the other hand, parameters Ra and φ are essential to reduce the occurrence of the low-temperature oxidation chemical reaction to reduce spontaneous combustion, which is detrimental to the climate. This study can be extended to the rectangular and spherical domains to investigate how heat transfer is affected by a multi-step combustion process.

Acknowledgments

The authors would like to acknowledge the Vaal University of Technology for providing facilities to produce this work

REFERENCES

[1] *A.T. Adeosun, S.O. Adesanya, R.S. Lebelo and J.A. Gbadeyan, "Mathematical investigation of a combustible viscoelastic material in a cylindrical stockpile with oxygen (O_2) consumption and induced electric field," Numerical Heat Transfer, Part B: Fundamentals, 2023, pp. 1-20.*

[2] *M.A. Taghikhani, "Power transformation insulation lifetime estimation methods," International Journal of Energy Engineering, Vol. 1 No. 1, 2011, pp. 9-11.*

[3] *S.R. Logan, "The origin and status of the Arrhenius equation," Journal of Chemical Education, vol. 59, no. 4, 1982, pp. 279–281.*

[4] *R.S. Lebelo, M. Waetzel, R.K. Mahlobo, K.C. Moloi and S.O. Adesanya, "On transient heat analysis of a two-step convective reactive cylinder," Journal of Physics: Conference Series, vol. 1730, 2021, pp. 1–5.*

[5] *R.S. Lebelo and O.D. Makinde, "Numerical investigation of CO_2 emission and thermal stability of a convective and radiative stockpile of reactive material in a cylindrical pipe," Advances in Mechanical Engineering, Vol. 7, No. 11, 2015, pp. 1–11.*

[6] *T. Chinyoka and O.D. Makinde, "Computational analysis of CO_2 emission, O_2 depletion and thermal decomposition in a cylindrical pipe filled with reactive materials," Communications in Nonlinear Science and Numerical Simulation, Vol. 18, 2023, pp. 2448-2461.*

[7] *R.S. Lebelo, "Thermal Conductivity Impact on Thermal Stability of Reactive Materials," Diffusion Forum, Vol. 11, 2017, pp 1-10.*

[8] *S. Lee, R. Chen and S. Volz, "Engineering and understanding of thermal conduction in materials," Journal of Applied Physics, Vol. 132 (040401), 2022, pp. 1-4.*

[9] *Eastman Therminol® heat transfer fluids, Heat transfer fluids by application, available at https://www.therminol.com/applications*

[10] *R.S. Lebelo and R.B. Mabuza, "Numerical Investigation of Thermal Stability in Media of Different Physical Geometries," Journal of Engineering and Applied Sciences, Vol. 12 (24), 2017, pp. 7555-7561.*

[11] *R.S. Lebelo, R.K. Mahlobo and S.O. Adesanya, "Investigating Thermal Stability in a Two-Step*
Convective Radiating Cylindrical Pipe," Defect and Diffusion Forum, Vol. 408, 2021, pp. 99-107.

[12] *R.S. Lebelo, K.C. Moloi, C.C. Chitumwa, M.W.R. Sadiki and P. Baloyi, "Steady-state Heat Transit Analysis in a Spherical Domain," in Proceedings of the 11th South African Conference on Computational and Applied Mechanics, SACAM 2018, 17-19 September 2018, Vanderbijlpark, South Africa (2018).*

[13] *O.S. Makinde, K.S. Adegbie and O.A. Fasoranbaku, "Mathematical modelling of two-step exothermic reactions with and without reactants consumption," FUTA Journal of Research in Sciences, Vol. 1, 2013, pp. 44-53.*